MOLECULAR IMAGING AND BIOLOGY

Mol Imaging Biol (2018) 20:388–397
DOI: 10.1007/s11307-017-1150-2

Published Online: 18 December 2017

RESEARCH ARTICLE

Metformin Promotes 2-Deoxy-2-[^{18}F]Fluoro-D-Glucose Uptake in Hepatocellular Carcinoma Cells Through FoxO1-Mediated Downregulation of Glucose-6-Phosphatase

Zhengjie Wang,[1] Fei Kang,[1] Yongheng Gao,[1] Yi Liu,[1] Xiaolong Xu,[2] Xiaowei Ma,[1] Wenhui Ma,[1] Weidong Yang,[1] Jing Wang[1]

[1]*Department of Nuclear Medicine, Xijing Hospital, Fourth Military Medical University, No.127 West Changle Road, Xi'an, 710032, People's Republic of China*

[2]*Department of Orthopaedics, Xijing Hospital, Fourth Military Medical University, No.127 West Changle Road, Xi'an, 710032, People's Republic of China*

Abstract

Purpose: The early diagnosis of primary hepatocellular carcinoma (HCC) has the potential to lead to significant improvements for the treatment and survival rates of cancer patients. 2-Deoxy-2-[^{18}F]fluoro-D-glucose ([^{18}F]FDG) is often used as a tracer for positive emission tomography (PET) and X-ray computed tomography (CT) imaging of cancer cells; however, [^{18}F]FDG PET/CT cannot currently be used as an early diagnostic technique for HCC. This is because these cancer cells express high levels of glucose-6-phosphatase (G6Pase) that is responsible for poor cellular retention of [^{18}F]FDG. Here, we sought to investigate the feasibility of metformin treatment to promote [^{18}F]FDG uptake in HCC and the mechanism involved.

Procedures: Human SMMC-7721 HCC cells were treated with metformin (up to 10 mM) or FoxO1 siRNA. The transcriptional and expression levels of FoxO1 and G6Pase were determined by quantitative RT-PCR and Western blotting, respectively. The feasibility of using metformin to promote [^{18}F]FDG uptake was investigated by both *in vitro* cell uptake analysis and *in vivo* microPET/CT imaging. Stable doxycycline-inducible cell lines with FoxO1-overexpression (FoxO1-OE) and FoxO1-knockdown (FoxO1-KD) were constructed to evaluate the impact of FoxO1 on G6Pase expression *in vitro* and [^{18}F]FDG uptake *in vivo*.

Results: Treatment of HCC cells with metformin (Met) leads to a dose-dependent reduction in the expression levels of FoxO1 at the protein level, but not at the mRNA level. Met-induced phosphorylation of FoxO1 initiates a reduction in the expression levels of G6Pase mRNA, which results in an overall increase in the uptake of [^{18}F]FDG into HCC cells and tumors.

Zhengjie Wang and Fei Kang contributed equally to this work.
Fei Kang and Jing Wang also contributed equally to this work.
Electronic supplementary material The online version of this article (https://doi.org/10.1007/s11307-017-1150-2) contains supplementary material, which is available to authorized users.

Correspondence to: Fei Kang; *e-mail:* fmmukf@qq.com, Jing Wang; *e-mail:* wangjing@fmmu.edu.cn

Conclusions: We propose that treatment of HCC cells with Met may be a useful strategy for improving the efficacy of [^{18}F]FDG as a tracer for PET/CT imaging of HCC tumors in patients.

Key Words: Metformin, FoxO1, G6Pase, Hepatocellular carcinoma, ^{18}F-FDG PET imaging

Introduction

Hepatocellular carcinoma (HCC) is the second highest cause of death from cancer worldwide, ranking as the third biggest cause of cancer mortality in China [1, 2]. The 5-year survival rates for early-stage HCC patients average around 70 %; however, the median survival period for advanced HCC patients is normally less than a year [3]. Hence, early diagnosis is crucial to improve the treatment of patients with HCC and increase their survival chances. Currently, the National Comprehensive Cancer Network (NCCN) guidelines recommend the use of four-phase X-ray computed tomography (CT) and dynamic magnetic resonance imaging (MRI) for the diagnosis of HCC [4]. However, the low sensitivity of these techniques (62.0–78.4 %), especially for the diagnosis of small tumors (≤ 2 cm^3), means that these approaches are not suitable as early diagnostic techniques for HCC [5].

Positron emission tomography (PET) using 2-deoxy-2-[^{18}F]fluoro-D-glucose ([^{18}F]FDG) as a tracer in combination with CT imaging is recognized as being a superior approach to traditional anatomical imaging for the early diagnosis and location of malignant tumors [6–8]. However, the accumulation levels of [^{18}F]FDG in HCC cells are often low, especially in differentiated HCC cells [9], which means that [^{18}F]FDG PET/CT imaging is not currently recommended as a diagnostic technique for HCC tumors [10].

[^{18}F]FDG is transported into cells by glucose transporter 1 (GLUT1), where it is then phosphorylated by hexokinase 2 (HK2) to afford charged [^{18}F]FDG-6-phosphate that accumulates within the cell. HCC tumors are known to overexpress the enzyme glucose 6-phosphatase (G6Pase) [11, 12], which can hydrolyze [^{18}F]FDG-6-phosphate to [^{18}F]FDG that may then be transported back out of cancer cells by glucose transporters and *P*-glycoproteins [13, 14]. Therefore, selective inhibition of G6Pase activity could potentially result in higher concentrations of [^{18}F]FDG accumulating in HCC cells, which would then allow PET/CT imaging to be used for the diagnosis of HCC tumors.

Metformin (Met) is used for the treatment of type 2 diabetes, where it is known to exert a range of pharmacologic effects on cellular glucose metabolism in both healthy and cancer cells [15, 16]. Met is thought to effectively downregulate G6Pase by reducing its mRNA expression levels [17]. Forkhead box protein O1 (FoxO1) is a transcription factor that plays an important role in regulating glucose metabolism and tumor progression [18, 19]. In its non-phosphorylated state, FoxO1 increases the rate of production of hepatic glucose by triggering an increase in the transcription levels of G6Pase [18]. Studies have shown that inhibition of FoxO1 activity can reduce the expression levels of G6Pase in the liver [20], with Met also having been reported to have a strong inhibitory effect on FoxO1 expression in macrophages [21]. Consequently, it was decided to investigate whether the treatment of HCC cells with Met would result in an increase in their overall [^{18}F]FDG uptake.

Materials and Methods

Cell Lines and Culture Conditions

Human differentiated hepatocellular carcinoma cells (SMMC-7721, obtained from the Chinese Center for Type Culture Collection) were cultured in RPMI-1640 media (Hyclone, Utah, USA) and 10 % FBS (Hyclone) in a humidified atmosphere containing 5 % CO_2 at 37 °C.

In Vitro Pharmacological Interventions

In vitro studies were carried out using HCC cells seeded into six-well plates at a concentration of 5×10^5 cells per well which were then treated with Met dissolved in RPMI-1640 at a concentration of 0 (negative control, NC), 1, 5, and 10 mM. Three replicates were carried out for each concentration of Met. Total RNA and protein levels were determined after 48 h using Western blotting analysis and quantitative real-time RT-PCR.

RNAi and Quantitative Real-Time RT-PCR

For *in vitro* RNAi studies, cells were transfected with either 100 nM siRNA targeted against FoxO1, fwd-5'-GGUUUGUACUGUUAUUAAA-3′, rev-5'-UUUAAUAACAGUACAAACC-3′ (Cell Signaling Technologies, Billerica, MA, USA), or negative control sequences using Lipofectamine 2000 (Invitrogen, Lake Placid, USA), as per manufacturer's instructions. The efficiency of these protocols was confirmed using a preliminary control experiment, as described in Suppl. Fig. 1 in the electronic supplementary material (ESM).

Total RNA was isolated from cells using a total RNA kit I(Omega Bio-Tek, GA, USA) according to the manufacturer's guidelines. Single-stranded cDNA was synthesized from total RNA using the PrimeScript™ RT Master Mix (TaKaRa, Dalian, China). Real time RT-PCR for each target was performed using SYBR® Premix Ex Taq II (TaKaRa).

The primer sets used were, for FoxO1, (5'-TTTGGACT GCTTCTCTCAGTTCCTGC-3′) and (5'-TTTGACAA TGTGTTGCCCAACCAAAG-3′); for G6Pase, (5'-GTGTCCGTGATCGCAGACC-3′) and (5'-GACGAGGT TGAGCCAGTCTC-3′); and for β-actin, (5'-TGGCACCC AGCACAATGAA-3′) and (5′-CTAAGTCATAGTCC GCCTAGAAGCA-3′). Thermal cycling conditions were set as follows: pre-heating (30 s at 94 °C) and 40 cycles of denaturation (10 s at 94 °C), annealing (30 s at 61 °C), and elongation (20 s at 72 °C). mRNA levels were normalized using a β-actin mRNA internal control.

Western Blot Analysis

Protein samples were quantified using a bicinchoninic acid assay kit (BCA; Boster, Hubei, China) employing 40 μg of protein from each sample. These samples were loaded onto 10 % sodium dodecyl sulfate-polyacrylamide 1-mm gels and transferred onto nitrocellulose membranes. Membranes were blocked for 2 h using 5 % bovine serum albumin (BSA; Boster) at 4 °C. After overnight incubation at 4 °C with primary antibodies, each membrane sample was washed five times with Tris-buffered saline containing Tween-20 (TBST) for 5 min and then incubated for 1 h at room temperature (RT) with a secondary antibody. Blots were visualized using the enhanced chemiluminescence (ECL) (Cell Signaling Technologies) method. Images were captured and analyzed using ImageJ software (National Institutes of Health). Relative expression levels were quantified by comparing band intensities with β-actin and normalized to controls. Statistical analysis was performed on three repeats.

The following primary antibodies were used (Cell Signaling Technologies): anti-phospho-AMP-activated protein kinase (AMPK) (Thr172), AMPK, phospho-protein kinase B (Akt) (Ser473), Akt, anti-eukaryotic translation initiation factor 4E-binding protein 1 (4EBP1), and phospho-4EBP1 (Ser65). Primary antibodies obtained from Abcam (USA) were FoxO1A, phospho-FoxO1A (Ser256), G6Pase, GLUT1, HK2, and ß-actin. Secondary anti-rabbit IgG antibody was obtained from BBI Life Sciences (Shanghai, China).

In Vitro [^{18}F]FDG Uptake Assay

[^{18}F]FDG cell uptake rate was measured according to previous studies [22]. SMC7721 cells were seeded at 2×10^4 cells/well in 24-well plates and treated with Met or FoxO1 siRNA for 48 h, carrying out three replicates for each experiment. For cell uptake studies, 500 μl (37 kBq) of [^{18}F]FDG in RPMI-1640 media without FBS was added to each tube. A tube containing 5 μl (0.37 kBq) of [^{18}F]FDG was prepared as a 1 % uptake reference. After incubation at 37 °C for 60 min, three washes were performed using ice-cold phosphate-buffered saline (PBS). Cells were digested with 500 μl 0.05 % trypsin, and contents were collected in a plastic tube. The radioactivity of the cells and the reference tube was determined using a γ-counter (Capintec, NJ, USA). Radiotracer uptake was corrected for decay, cell count, and percentage of retained activity per 5×10^5 cells.

Generation of Doxycycline-Inducible FoxO1-Manipulating Stable Cell Lines

Inducible lentivirus expressing FoxO1 siRNA (FoxO1-KD) and lentivirus overexpressing FoxO1 (FoxO1-OE) under the control of a doxycycline-dependent Tet On/Tet Off switch were constructed by Genechem (Shanghai, China). According to the manufacturer's experimental protocol, 2 μg/ml puromycin (Sigma Aldrich, St. Louis, MO, USA) was applied 72 h after transfection and then allowed to stand for 48 h before being used as a stably transfected cell line clone. For *in vitro* doxycycline (Dox) (Sigma Aldrich) induction, stably transfected cells were plated into six-well plates at a concentration of 5×10^5 cells per well and treated with Dox (5 μg/ml), Met (10 mM), or Met (10 mM) + Dox (5 μg/ml). Total RNA and protein were extracted, and their values were determined after 48 h.

In Vivo Tumor Xenograft Studies

BALB/c nude mice were obtained from the Medical Laboratory Animal Department of the Fourth Military Medical University. For inoculation, 6×10^6 cells suspended in 100 μl of PBS were subcutaneously injected into the right flank of six-week-old male nude mice weighing 20–25 g. Over 3 weeks of observation, xenograft tumors reached a volume of around 100 mm^3. Animal models bearing FoxO1-KD tumors were randomly divided into two groups ($n = 5$ mice per group) and treated with Met (250 mg/kg/day) intraperitoneally [16] and Dox 0.2 ml (2 mg/ml) by gavage [23] for 2 days. The nude mice bearing FoxO1-OE tumors ($n = 5$) were treated with Met for 2 days and Dox plus Met for another 2 days. All mice were kept under non-fasting conditions and were housed at a constant RT of 21 °C to avoid the influence of any external factors on glucose or [^{18}F]FDG uptake.

[^{18}F]FDG Micro-PET/CT Imaging

Before pharmacological interventions, 150–200 μCi of [^{18}F]FDG in 150 μl of saline was intraperitoneally injected into each tumor-bearing mouse. The PET/CT data acquisition procedure was performed 1 h after [^{18}F]FDG injection, using a small-animal PET/CT system (Mediso). Once anesthesia had been induced, the mice were

anesthetized using a cone-shaped face mask to continuously deliver isoflurane (2 %) at a flow rate of 1.5 l/min. An electric heating pad was placed under the animal to help maintain body temperature using a small-animal PET/CT system. PET/CT data were acquired for 600 s for each mouse under continuous anesthesia. After imaging, mice were treated with Met and/or Dox and re-imaged using the same protocol after 48 h. All PET/CT images were processed and analyzed using NuclinenanoScan software (Mediso). For semi-quantitative analysis, three-dimensional (3D) regions of interest were adjusted manually to define the borders of the tumor and were carefully drawn using the PET and CT images of each mouse. 3D regions of interest with a diameter of 1 cm were delineated on the liver as non-target (NT) references. Tracer uptake by the tumor and the liver tissue was quantified as standardized uptake values (SUVs) using the formula SUV = tissue activity concentration (Bq/ml)/injected dose (Bq) × body weight (g). The maximum tumor SUV, the T/NT ratio of the mean tumor SUV, and the mean NT SUV were calculated and compared by comparison of data from different interventions.

Immunohistochemistry Analysis

Each tumor was harvested from mice models and fixed with 10 % formalin. These formalin-fixed, paraffin embedded tissue blocks were then cut serially into 3-mm-thick sections that were dewaxed in xylene and rehydrated by exposure to a graded series of ethanol solutions. After three washes in PBS, heat-induced antigen was retrieved in 0.01 M citric acid buffer (pH 6.0) and autoclaved for 5 min at 120 °C. Non-specific binding sites were blocked through pre-incubation with normal bovine serum for 30 min. Slices were washed three times in PBS for 5 min between each wash. These tissue sections were then incubated with anti-G6Pase antibodies, anti-GLUT1 antibodies, or anti-HK2 antibodies, followed by treatment with horseradish peroxidase-conjugated anti-rabbit IgG. In all experiments, positive cells were visualized using 3,3-diaminobenzidine tetrahydrochloride (Shanghai Sangon), before being counterstained with hematoxylin.

Statistical Analysis

All values are expressed as mean ± SEM. Statistical analysis was performed using GraphPad Prism software. Differences between two groups were determined by Student's *t* test. A one-way ANOVA followed by *post hoc* Student-Newman-Keuls test was employed to analyze pairwise comparisons of every combination of multiple group pairs. *In vitro* experiments were repeated three times. A probability value of $P < 0.05$ was considered significant.

Results

Metformin Reduces the Expression Levels of FoxO1 at a Post-transcriptional Level

Studies on the treatment of FoxO1 with Met were carried out *in vitro*, with treatment of FoxO1 with FoxO1-knockdown siRNA being used as a control. As shown in Fig. 1b, c (using untreated controls as reference), the relative expression levels of FoxO1 were significantly reduced in both the 10 mM Met group (1.000 ± 0.058 *vs.* 0.561 ± 0.052, $P = 0.0048$) and the FoxO1-siRNA group (1.000 ± 0.058 *vs.* 0.495 ± 0.0232, $P = 0.0031$). However, as shown in Fig. 1a, the relative transcription levels of FoxO1 were not significantly altered in every group that was treated with Met ($F = 0.5684$, $P = 0.6512$), suggesting that Met reduces FoxO1 expression levels *via* a post-transcriptional regulatory mechanism.

To further understand this mechanism, the phosphorylation levels of both FoxO1 and the upstream AMPK-Akt-4EBP1 pathway that controls FoxO1 post-transcriptional expression levels were determined. As shown in Fig. 1d, the expression ratio of phosphorylated FoxO1 to total FoxO1 was unchanged in the treatment with 10 mM Met ($F = 0.1116$, $P = 0.9756$). However, the use of 10 mM Met did result in increased levels of phosphorylated AMPK (1.000 ± 0.0833 *vs.* 1.424 ± 0.3789, $P = 0.0097$), while the levels of phosphorylated Akt and phosphorylated 4EBP1 were decreased (1.000 ± 0.1217 *vs.* 0.3758 ± 0.0372, $P = 0.0083$; 1.000 ± 0.0752 *vs.* 0.364 ± 0.0347, $P = 0.0016$) (Fig. 2). This indicates that Met has an overall inhibitory effect on the AMPK-Akt-4EBP1 pathway.

Metformin Acts on FoxO1 to Control the Expression Levels of G6Pase

The effect of Met and FoxO1 on the expression of G6Pase and FoxO1-knockdown (FoxO1-KD) was investigated using siRNA and FoxO1-overexpressed (FoxO1-OE) using a Dox-inducible Tet on/Tet off switch system. As shown in Fig. 3a, the relative transcription levels of G6Pase were significantly reduced on treatment with Met (0 mM 1.000 ± 0.0893 *vs.* 1 mM Met 0.5271 ± 0.048, $P = 0.0096$; 5 mM Met 0.053 ± 0.0055, $P = 0.0005$; 10 mM Met 0.0448 ± 0.0068, $P = 0.0004$) and FoxO1-KD (0 mM 1.000 ± 0.0893 *vs.*0.0287 ± 0.0037, $P = 0.0004$). Figure 3b, c reveals that the relative expression level of G6Pase was also downregulated by treatment with Met (0 mM 1.000 ± 0.0921 *vs.* 1 mM Met 1.008 ± 0.1101, $P = 0.9602$; 5 mM Met 0.6655 ± 0.0652, $P = 0.0413$; 10 mM Met 0.5621 ± 0.0974, $P = 0.0309$) and FoxO1-KD (0 mM 1.000 ± 0.0921 *vs.* 0.4247 ± 0.0841, $P = 0.0099$).

FoxO1-OE manipulation using Dox increased the expression of FoxO1, resulting in increased transcription and expression of G6Pase (See Fig. 4). Additionally, the

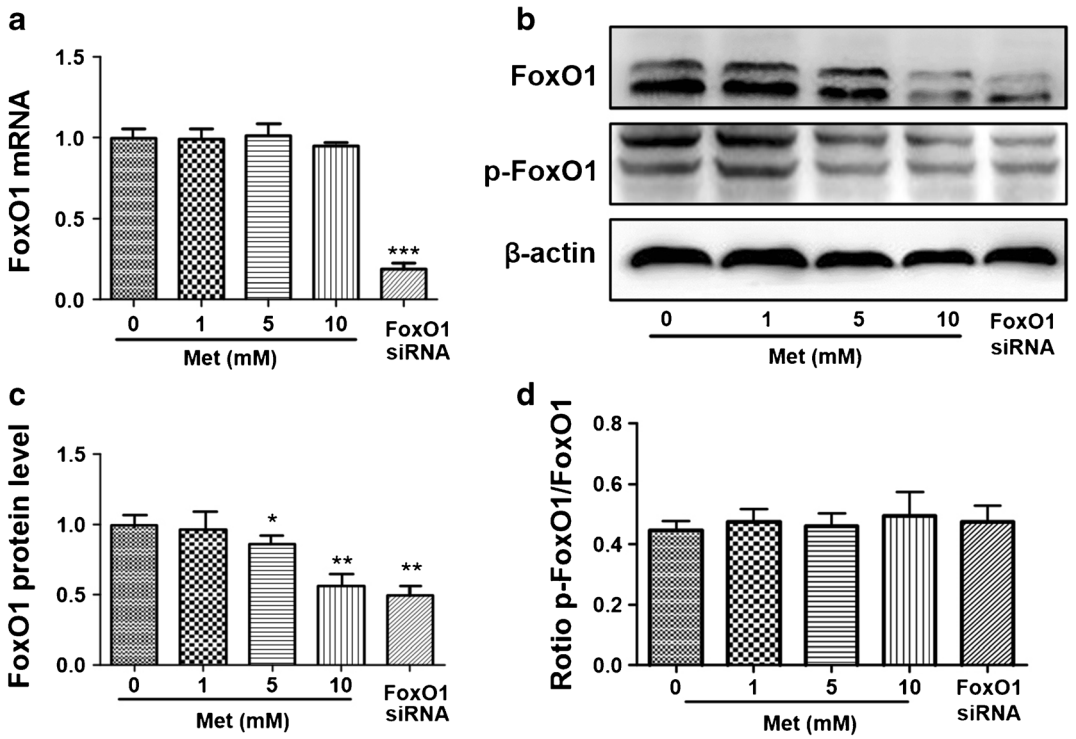

Fig. 1 Analysis of FoxO1 in SMMC-7721 cells after treatment with Met and transfection with FoxO1-siRNA. **a** FoxO1 mRNA levels determined by quantitative RT-PCR. **b** Expression levels of FoxO1 determined by Western blot. Semi-quantitative analysis of expression levels of **c** FoxO1 and **d** the ratio of p-FoxO1/FoxO1 expression levels. Relative expression levels determined by normalization of data relative to untreated controls to obtain relative expression levels. $^{*}P < 0.05$; $^{**}P < 0.01$; $^{***}P < 0.001$.

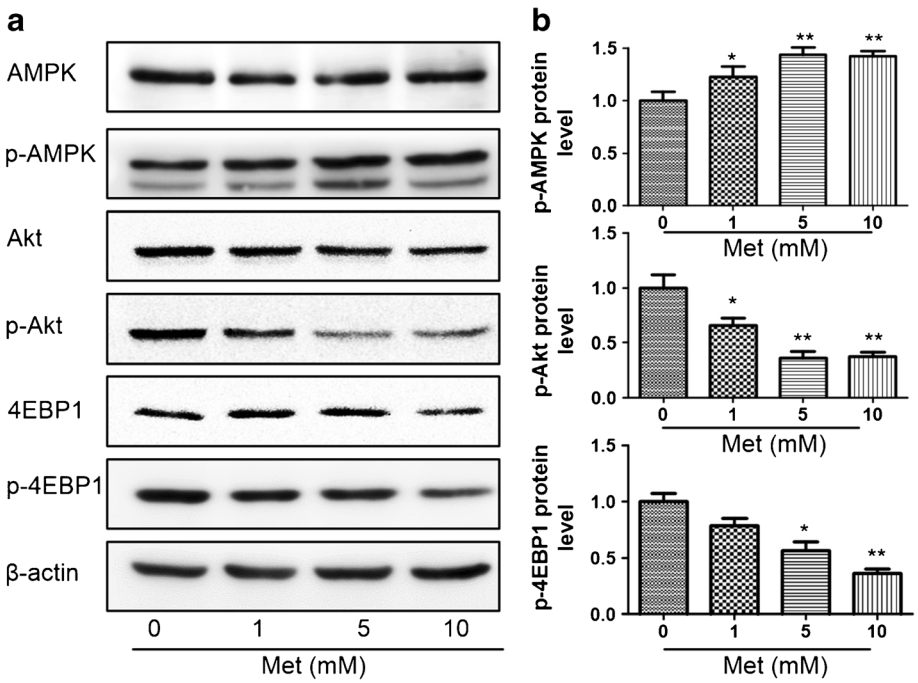

Fig. 2 Analysis of AMPK, Akt, and 4EBP1 in SMMC-7721 cells after Met treatment. **a** Expression levels of AMPK, Akt, and 4EBP1 determined by Western blot. **b** Semi-quantitative analysis of expression levels of AMPK, Akt, and 4EBP1. All data are normalized with respect to untreated controls to obtain relative expression levels. $^{*}P < 0.05$; $^{**}P < 0.01$; $^{***}P < 0.001$.

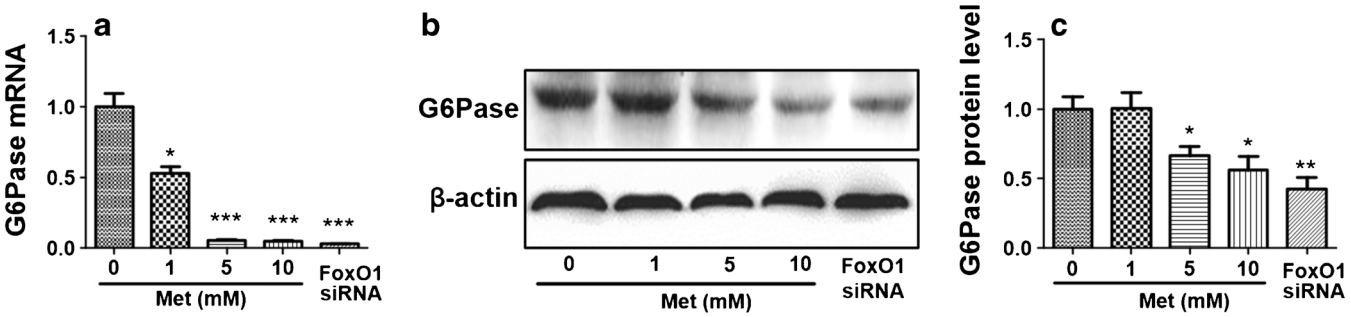

Fig. 3 Analysis of G6Pase in SMMC-7721 cells after Met treatment and FoxO1-siRNA treatment. **a** G6Pase mRNA levels determined by quantitative RT-PCR. **b** Expression levels of G6Pase determined by Western blot. **c** Semi-quantitative analysis of expression levels of G6Pase. All data are normalized with respect to untreated controls to obtain relative expression levels. $^{*}P < 0.05$; $^{**}P < 0.01$; $^{***}P < 0.001$.

combined intervention of Met and Dox partially rescued the positive effect of FoxO1-OE manipulation on FoxO1 (2.656 ± 0.0959 *vs.* 3.548 ± 0.1700, $P = 0.0038$) and G6Pase expression (1.323 ± 0.0492 *vs.* 2.177 ± 0.1348, $P = 0.0011$). This demonstrates that both Met and FoxO1 have a regulatory effect on the transcriptional and expression levels of G6Pase. Details of the transcriptional verification of the FoxO1-OE manipulation system are described in Suppl. Fig. 2 in ESM.

Treatment with Metformin and FoxO1 Inhibition Results in an Increase in the Intracellular Concentration of [^{18}F]FDG in HCC Cells

In vitro cell uptake assay and *in vivo* microPET/CT imaging studies were carried out to determine whether Met-induced alteration of G6Pase levels resulted in an increase in the uptake of [^{18}F]FDG in SMMC-7721 cells. As shown in Fig. 5, treatment with Met resulted in a dose-dependent

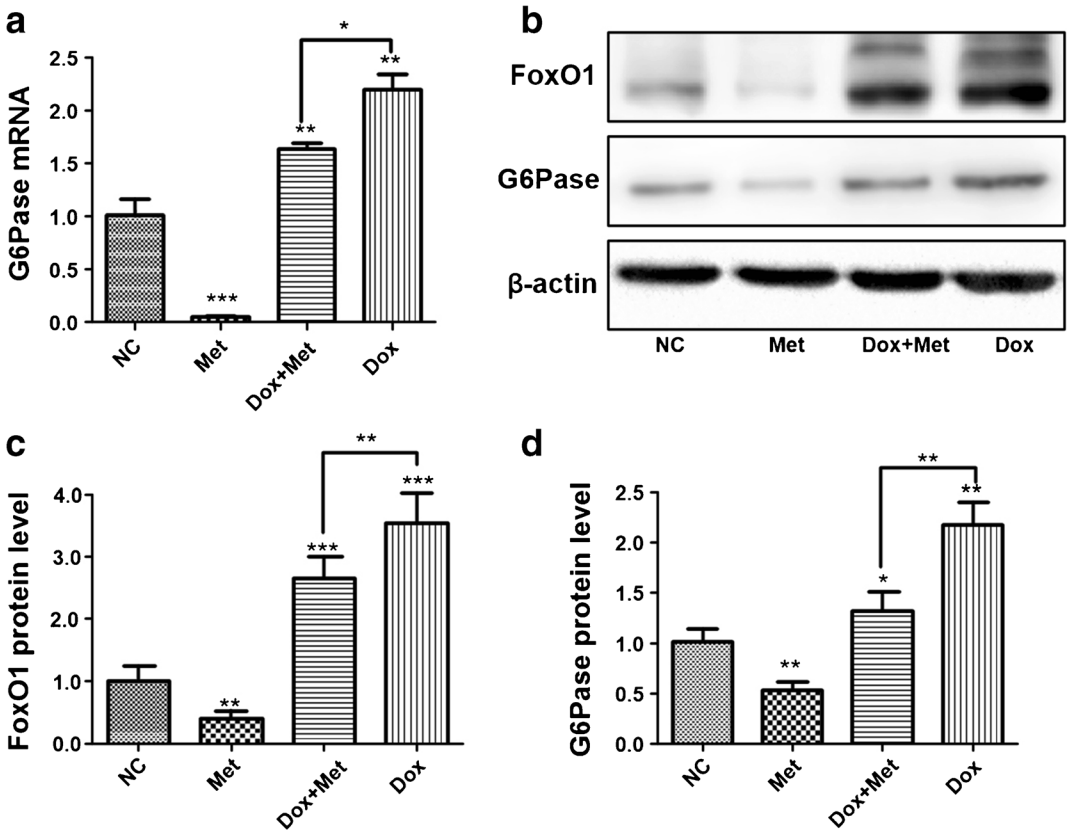

Fig. 4 *In vitro* analysis of G6Pase in stably transduced Dox-inducible FoxO1 overexpressing (FoxO1-OE) SMMC-7721 cells after treatment with Met and/or Dox. **a** G6Pase mRNA levels determined by quantitative RT-PCR. **b** Western blot of FoxO1 and G6Pase. Semi-quantitative analysis of expression levels of **c** FoxO1 and **d** G6Pase. All data are normalized to the results of the NC group to obtain relative expression levels. $^{*}P < 0.05$; $^{**}P < 0.01$; $^{***}P < 0.001$.

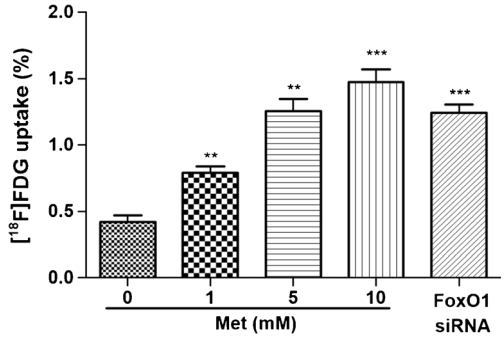

Fig. 5 *In vitro* analysis of [^{18}F]FDG uptake levels in SMMC-7721 cells after treatment with Met and FoxO1-siRNA. The results are corrected for radionuclide decay and presented as a percentage of initial activity taken up by 5×10^5 cells. $^{**}P < 0.01$; $^{**}P < 0.001$.

increase in the uptake of [^{18}F]FDG into HCC cells *in vitro*. The [^{18}F]FDG uptake ratio in SMMC-7721 cells was found to be 3.5-fold higher in the 10 mM Met group than in the untreated control group (1.474 ± 0.0946 *vs.* 0.421 ± 0.0487, $P = 0.0006$). Furthermore, the [^{18}F]FDG uptake ratio in the FoxO1-siRNA group was also found to be significantly higher than in the control group (1.244 ± 0.0630 *vs.* 0.421 ± 0.0487, $P = 0.0005$).

Met treatment of mice, bearing inducible FoxO1-KD or FoxO1-OE HCC tumors, also resulted in elevated [^{18}F]FDG uptake levels (see Fig. 6a, b). Figure 6c, d reveals that the SUV_{Max} value and T/NT ratios observed during NC imaging of Met-treated mice were significantly higher in both FoxO1-KD mice (SUV_{Max} value 1.907 ± 0.139 *vs.* 0.443 ± 0.022, $P = 0.0005$; T/NT ratio 3.678 ± 0.131 *vs.* 1.037 ± 0.0185, $P < 0.0001$) and FoxO1-OE mice (SUV_{Max} value 1.764 ± 0.057 *vs.* 0.407 ± 0.018, $P < 0.0001$; T/NT ratio 3.769 ± 0.098 *vs.* 1.019 ± 0.018, $P < 0.0001$). These findings confirm the *in vitro* results, demonstrating that the treatment with Met has a positive effect on the incorporation of [^{18}F]FDG into HCC cells *in vivo*.

Dox-induced knockout of FoxO1 in FoxO1-KD mice was also shown to result in a significant increase in the tumor uptake of [^{18}F]FDG (SUV_{Max} value 1.013 ± 0.055 *vs.* 0.443 ± 0.022, $P = 0.0006$; T/NT ratio: 3.065 ± 0.049 *vs.* 1.037 ± 0.0185, $P < 0.0001$). However, simultaneous overexpression of FoxO1 in FoxO1-OE mice did not result in Met having any positive effects on the uptake of [^{18}F]FDG into tumor cells (SUV_{Max} value 0.533 ± 0.064 *vs.* 1.764 ± 0.057, $P = 0.0001$; T/NT ratio 1.287 ± 0.099 *vs.* 3.769 ± 0.098, $P < 0.0001$). Taken together, these results confirm that FoxO1 plays an important role in regulating the rate of [^{18}F]FDG accumulation in HCC cells.

In the glycolytic pathway, [^{18}F]FDG is transported into cells by GLUT1 where HK2 then transforms it into [^{18}F]FDG-6-phosphate. In order to probe the mechanism of action of Met and FoxO1-KD in increasing intracellular levels of [^{18}F]FDG *in vivo*, it was decided to examine the expression levels of GLUT1, HK2, and G6Pase in tumor

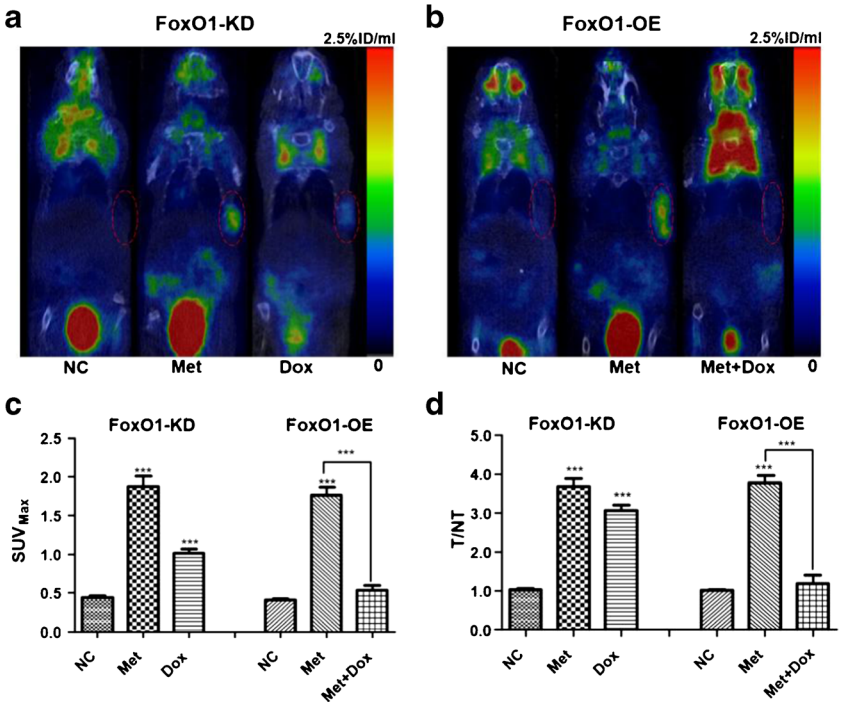

Fig. 6 PET of FoxO1-knockdown (FoxO1-KD) or FoxO1-overexpression (FoxO1-OE) SMMC-7721 tumors from BALB/c mice treated with Met and/or Dox. Representative coronal [^{18}F]FDG microPET/CT images of mouse models bearing **a** Dox-inducible FoxO1-KD or **b** FoxO1-OE SMMC-7721 tumors after treatment with Met and/or Dox. Tumors indicated by dashed circles. Analysis of **c** SUVMax and **d** T/NT (target/non-target) values of tumors in each intervention group. Homolateral liver tissue was defined using NT reference. $^{*}P < 0.05$; $^{**}P < 0.01$; $^{**}P < 0.001$.

cells. Western blot analysis of tumor tissues revealed a significant decrease in G6Pase expression in both Met-treated and FoxO1-KD mice. This decrease corresponded with the expression levels of GLUT1 and HK2 remaining unchanged for all groups studied, with immunohistochemical analysis also confirming these results (Suppl. Fig. 7 in ESM).

Furthermore, it was found that the treatment of healthy liver samples with Met (50 mg/kg/day) resulted in no change in SUV_{Max} and SUV_{mean} values (see Suppl. Fig. 4 in ESM) when compared to untreated samples (SUV_{Max} 0.360 ± 0.029 *vs.* 0.336 ± 0.050, $P = 0.7411$; SUV_{mean} 0.302 ± 0.019 *vs.* 0.313 ± 0.042, $P = 7983$). Therefore, in contrast to HCC cells, this implies that the treatment of healthy liver cells with Met results in no change in the rate of their [^{18}F]FDG uptake.

Discussion

This study has shown that the treatment of HCC cells with Met results in intracellular accumulation of [^{18}F]FDG, *via* a process that is controlled by the AMPK-Akt-4EBP1 pathway and the FoxO1 transcription factor. It has been found that the treatment of HCC cells with Met significantly increases the uptake of [^{18}F]FDG by ~3.5-fold *in vitro* and ~5-fold *in vivo*. This increase in intracellular concentration of [^{18}F]FDG in HCC cells is triggered by the transcriptional downregulation of G6Pase that arises from Met-mediated phosphorylation of the FoxO1 transcription factor that is downregulated by the action of the AMPK-Akt-4EBP1 pathway.

It has previously been reported that Met can be used to promote the accumulation of [^{18}F]FDG in normal intestinal cells [24, 25], while Habibollahi et al. have described that Met increases [^{18}F]FDG uptake in a colon cancer mouse model *via* AMPK-mediated changes [22]. Mashhedi et al. have demonstrated that Met decreases [^{18}F]FDG uptake in colon cancer under certain conditions [26], while a negative effect for Met on [^{18}F]FDG uptake in thyroid cancer cells was recently reported [27]. In this study, we have shown that Met has a positive effect on [^{18}F]FDG uptake in HCC cells; therefore, it is clear that Met may play different roles in controlling glycometabolism in different tumor cell types.

This study has also revealed that Met reduces the post-transcriptional expression of FoxO1, which is consistent with previous studies reported on the activity of FoxO1 in endothelial cells and diabetic animal models [28, 29]. We have also discovered the inhibitory effect of Met on the AMPK-Akt-4EBP1 signaling pathway. 4EBP1 is a key regulator of eIF4E, which is a key rate-limiting component of the eukaryotic translation mechanism that controls the post-transcriptional translation of FoxO1. We have shown that the ratio of phosphorylated FoxO1 to total FoxO1 is not altered in the treatment with Met. It was reported that both Akt [30] and Met [21] could increase the levels of p-FoxO1, while in our study, we found that Met decreased the expression levels of both Akt and p-FoxO1, with the ratio of p-FoxO1/FoxO1 remaining unchanged. These results indicate that the main role of Met is to reduce the overall levels of p-FoxO1 and FoxO1 through the inhibition of the AMPK-Akt-4EBP1 pathway.

The rate of [^{18}F]FDG uptake into cells is primarily determined by the expression levels of GLUT1 and HK2 [31], with previous studies having shown that the expression levels of GLUT1 in adipocytes and heart muscle cells are increased in the presence of Met [32, 33]. However, we have found that the treatment of SMMC7721 cells with metformin does not significantly alter their GLUT1 expression levels. Furthermore, consistent with previous studies [34], we have found that metformin does not change HK2 expression levels in SMMC7721 cells, either *in vitro* (Suppl Fig. 5, in ESM) or *in vivo*. Therefore, our results indicate that metformin and FoxO1-KD increase [^{18}F]FDG uptake in SMMC-7721 cells primarily by reducing the expression levels of G6Pase.

There are many tracers that can be used for HCC PET imaging applications. These include [^{11}C]choline, [^{18}F]fluoroethylcholine, and [^{11}C]acetate, which have all been proposed as effective tracers for the early detection of HCC [35–38]. However, the performance of these tracers for the diagnosis of poorly differentiated HCC has been shown to be inferior to PET/CT imaging using [^{18}F]FDG [37]. We have shown that Met can increase the amount of [^{18}F]FDG that is incorporated into HCC cells and tumors, while Met does not increase the uptake of [^{18}F]FDG into normal liver cells [39]. The effective Met dosage used in our mice studies was 250 mg/kg/day, which corresponds to a theoretical required dosage of 20.8 mg/kg/day in humans, which is below the limiting dosage approved for use in human of 2000 mg/day [40]. Therefore, we propose that our Met approach to enhance [^{18}F]FDG uptake may represent a safe and effective improvement for the PET/CT imaging of HCC cells using [^{18}F]FDG as an imaging agent.

This study has some limitations. Firstly, while both SMMC-7721 and HepG2 (Suppl. Fig. 6 in ESM) HCC cell lines were investigated *in vitro*, HepG2 cell lines are not tumorigenic in immunosuppressed mice and so our study only demonstrated that 18F-FDG uptake in SMMC-7721 cells was significantly elevated by metformin treatment *in vivo*. Future work should aim to determine whether Met can be used to increase levels of 18F-FDG in other types of HCC cell line *in vivo*, which will require new clinical 18F-FDG PET/CT protocols for the imaging of HCC tumors to be established. Secondly, a xenograft mouse flank model has been used in this study; however, it is known that there are significant differences in gene expression of key enzymes between human and mice liver [41]. Consequently, we intend to carry out further studies using human hepatocytes implanted on the other flank such as NT which will allow for contrast uptake between well-differentiated HCC and surrounding liver tissues to be observed.

Conclusion

Metformin can significantly increase the uptake of [^{18}F]FDG in SMMC-7721 HCC cells *in vitro* and *in vivo*, by decreasing G6Pase expression. FoxO1 is a key factor that mediates the regulation of G6Pase and [^{18}F]FDG uptake by metformin. Metformin treatment and FoxO1 inhibition may be potential strategies to improve the performance of [^{18}F]FDG PET/CT in early detection of HCC.

Acknowledgments. We thank Yongzhan Nie from the State Key Laboratory of Cancer Biology (Xi'an, China) for their generous support and Liwen Li and Mingxuan Zhao for their technical assistance in conducting this research.

Compliance with Ethical Standards. Experiments were performed in accordance with the ethically approved animal experimental guidelines of the Medical Laboratory Animal Department of the Fourth Military Medical University.

Conflict of Interest

The authors declare that they have no conflict of interest.

References

1. Chen W, Zheng R, Baade PD, Zhang S, Zeng H, Bray F, Jemal A, Yu XQ, He J (2016) Cancer statistics in China, 2015. CA Cancer J Clinicians 66(2):115–132. https://doi.org/10.3322/caac.21338
2. Torre LA, Bray F, Siegel RL et al (2015) Global cancer statistics, 2012. CA: Canc J Clinicians 65:87–108
3. Padhya KT, Marrero JA, Singal AG (2013) Recent advances in the treatment of hepatocellular carcinoma. Curr Opin Gastroenterol 29(3):285–292. https://doi.org/10.1097/MOG.0b013e32835ff1cf
4. Llovet JM, Ducreux M, Lencioni R et al (2012) EASL-EORTC clinical practice guidelines: management of hepatocellular carcinoma. Eur J Cancer 48:599–641
5. Kwon HJ, Byun JH, Kim JY, Hong GS, Won HJ, Shin YM, Kim PN (2015) Differentiation of small (≤2 cm) hepatocellular carcinomas from small benign nodules in cirrhotic liver on gadoxetic acid-enhanced and diffusion-weighted magnetic resonance images. Abdom Imaging 40(1):64–75. https://doi.org/10.1007/s00261-014-0188-8
6. Groheux D, Espie M, Giacchetti S et al (2013) Performance of FDG PET/CT in the clinical management of breast cancer. Radiology 266(2):388–405. https://doi.org/10.1148/radiol.12110853
7. Bar-Shalom R, Yefremov N, Guralnik L, Gaitini D, Frenkel A, Kuten A, Altman H, Keidar Z, Israel O (2003) Clinical performance of PET/CT in evaluation of cancer: additional value for diagnostic imaging and patient management. J Nucl Med 44(8):1200–1209
8. Lardinois D, Weder W, Hany TF, Kamel EM, Korom S, Seifert B, von Schulthess GK, Steinert HC (2003) Staging of non-small-cell lung cancer with integrated positron-emission tomography and computed tomography. N Engl J Med 348(25):2500–2507. https://doi.org/10.1056/NEJMoa022136
9. Park JW, Kim JH, Kim SK, Kang KW, Park KW, Choi JI, Lee WJ, Kim CM, Nam BH (2008) A prospective evaluation of ^{18}F-FDG and 11C-acetate PET/CT for detection of primary and metastatic hepatocellular carcinoma. J Nucl Med 49(12):1912–1921. https://doi.org/10.2967/jnumed.108.055087
10. Benson AR, D'Angelica MI, Abbott DE et al (2017) NCCN guidelines insights: hepatobiliary cancers, version 1.2017. J Natl Compr Cancer Netw 15(5):563–573. https://doi.org/10.6004/jnccn.2017.0059
11. Izuishi K, Yamamoto Y, Mori H et al (2014) Molecular mechanisms of [18F]fluorodeoxyglucose accumulation in liver cancer. Oncol Rep 31(2):701–706. https://doi.org/10.3892/or.2013.2886
12. Okazumi S, Isono K, Enomoto K, Kikuchi T, Ozaki M, Yamamoto H, Hayashi H, Asano T, Ryu M (1992) Evaluation of liver tumors using fluorine-18-fluorodeoxyglucose PET: characterization of tumor and assessment of effect of treatment. J Nucl Med 33(3):333–339
13. Lorke DE, Kruger M, Buchert R et al (2001) In vitro and in vivo tracer characteristics of an established multidrug-resistant human colon cancer cell line. J Nucl Med 42(4):646–654
14. Yu C, Wan W, Zhang B et al (2012) Evaluation of the relationship between [^{18}F]FDG and P-glycoprotein expression: an experimental study. Nuclr Med Biol 39:671–678
15. Zhang ZJ, Zheng ZJ, Shi R, Su Q, Jiang Q, Kip KE (2012) Metformin for liver cancer prevention in patients with type 2 diabetes: a systematic review and meta-analysis. J Clin Endocrinol Metab 97(7):2347–2353. https://doi.org/10.1210/jc.2012-1267
16. Qu Z, Zhang Y, Liao M, Chen Y, Zhao J, Pan Y (2012) In vitro and in vivo antitumoral action of metformin on hepatocellular carcinoma. Hepatol Res 42(9):922–933. https://doi.org/10.1111/j.1872-034X.2012.01007.x
17. Heishi M, Hayashi K, Ichihara J, Ishikawa H, Kawamura T, Kanaoka M, Taiji M, Kimura T (2008) Comparison of gene expression changes induced by biguanides in db/db mice liver. J Toxicol Sci 33(3):339–347. https://doi.org/10.2131/jts.33.339
18. Zhang X, Tang N, Hadden TJ, Rishi AK (2011) Akt, FoxO and regulation of apoptosis. Biochim Biophys Acta 1813(11):1978–1986. https://doi.org/10.1016/j.bbamcr.2011.03.010
19. O-Sullivan I, Zhang W, Wasserman DH et al (2015) FoxO1 integrates direct and indirect effects of insulin on hepatic glucose production and glucose utilization. Nature Comm 6:7079. https://doi.org/10.1038/ncomms8079
20. Samuel VT, Choi CS, Phillips TG, Romanelli AJ, Geisler JG, Bhanot S, McKay R, Monia B, Shutter JR, Lindberg RA, Shulman GI, Veniant MM (2006) Targeting foxo1 in mice using antisense oligonucleotide improves hepatic and peripheral insulin action. Diabetes 55(7):2042–2050. https://doi.org/10.2337/db05-0705
21. Song J, Ren P, Zhang L, Wang XL, Chen L, Shen YH (2010) Metformin reduces lipid accumulation in macrophages by inhibiting FOXO1-mediated transcription of fatty acid-binding protein 4. Biochem Biophys Res Comm 393(1):89–94. https://doi.org/10.1016/j.bbrc.2010.01.086
22. Habibollahi P, van den Berg NS, Kuruppu D, Loda M, Mahmood U (2013) Metformin—an adjunct antineoplastic therapy—divergently modulates tumor metabolism and proliferation, interfering with early response prediction by ^{18}F-FDG PET imaging. J Nucl Med 54(2):252–258. https://doi.org/10.2967/jnumed.112.107011
23. Cawthorne C, Swindell R, Stratford IJ, Dive C, Welman A (2007) Comparison of doxycycline delivery methods for Tet-inducible gene expression in a subcutaneous xenograft model. J Biomol Tech 18(2):120–123
24. JR O, Song HC, Chong A et al (2010) Impact of medication discontinuation on increased intestinal FDG accumulation in diabetic patients treated with metformin. AJR Am J Roentgenol 195:1404–1410
25. Massollo M, Marini C, Brignone M, Emionite L, Salani B, Riondato M, Capitanio S, Fiz F, Democrito A, Amaro A, Morbelli S, Piana M, Maggi D, Cilli M, Pfeffer U, Sambuceti G (2013) Metformin temporal and localized effects on gut glucose metabolism assessed using ^{18}F-FDG PET in mice. J Nucl Med 54(2):259–266. https://doi.org/10.2967/jnumed.112.106666
26. Mashhedi H, Blouin MJ, Zakikhani M, David S, Zhao Y, Bazile M, Birman E, Algire C, Aliaga A, Bedell BJ, Pollak M (2011) Metformin abolishes increased tumor ^{18}F-2-fluoro-2-deoxy-D-glucose uptake associated with a high energy diet. Cell Cycle 10(16):2770–2778. https://doi.org/10.4161/cc.10.16.16219
27. Shen CT, Wei WJ, Qiu ZL, Song HJ, Zhang XY, Sun ZK, Luo QY (2017) Metformin reduces glycometabolism of papillary thyroid carcinoma in vitro and in vivo. J Mol Endocrinol 58(1):15–23. https://doi.org/10.1530/JME-16-0134
28. Nagashima T, Shigematsu N, Maruki R, Urano Y, Tanaka H, Shimaya A, Shimokawa T, Shibasaki M (2010) Discovery of novel forkhead box O1 inhibitors for treating type 2 diabetes: improvement of fasting glycemia in diabetic db/db mice. Mol Pharmacol 78(5):961–970. https://doi.org/10.1124/mol.110.065714
29. Li X, Kover KL, Heruth DP, Watkins DJ, Moore WV, Jackson K, Zang M, Clements MA, Yan Y (2015) New insight into metformin action: regulation of ChREBP and FOXO1 activities in endothelial cells. Mol Endocrinol 29(8):1184–1194. https://doi.org/10.1210/ME.2015-1090
30. Wang Y, Zhou Y, Graves DT (2014) FOXO transcription factors: their clinical significance and regulation. Biomed Res Int 2014:925350

31. Gallagher BM, Fowler JS, Gutterson NI, MacGregor RR, Wan CN, Wolf AP (1978) Metabolic trapping as a principle of oradiopharmaceutical design: some factors resposible for the biodistribution of [^{18}F] 2-deoxy-2-fluoro-D-glucose. J Nucl Med 19(10):1154–1161
32. Matthaei S, Greten H (1991) Evidence that metformin ameliorates cellular insulin-resistance by potentiating insulin-induced translocation of glucose transporters to the plasma membrane. Diabete Metab 17(1 Pt 2):150–158
33. Fischer Y, Thomas J, Rosen P et al (1995) Action of metformin on glucose transport and glucose transporter GLUT1 and GLUT4 in heart muscle cells from healthy and diabetic rats. Endocrinology 136(2):412–420. https://doi.org/10.1210/endo.136.2.7835271
34. Salani B, Ravera S, Amaro A, Salis A, Passalacqua M, Millo E, Damonte G, Marini C, Pfeffer U, Sambuceti G, Cordera R, Maggi D (2015) IGF1 regulates PKM2 function through Akt phosphorylation. Cell Cycle 14(10):1559–1567. https://doi.org/10.1080/15384101.2015.1026490
35. Yamamoto Y, Nishiyama Y, Kameyama R, Okano K, Kashiwagi H, Deguchi A, Kaji M, Ohkawa M (2008) Detection of hepatocellular carcinoma using ^{11}C-choline PET: comparison with ^{18}F-FDG PET. J Nucl Med 49(8):1245–1248. https://doi.org/10.2967/jnumed.108.052639
36. Kolthammer JA, Corn DJ, Tenley N, Wu C, Tian H, Wang Y, Lee Z (2011) PET imaging of hepatocellular carcinoma with ^{18}F-fluoroethylcholine and ^{11}C-choline. Eur J Nucl Med Mol Imaging 38(7):1248–1256. https://doi.org/10.1007/s00259-011-1743-y
37. Bertagna F, Bertoli M, Bosio G, Biasiotto G, Sadeghi R, Giubbini R, Treglia G (2014) Diagnostic role of radiolabelled choline PET or PET/CT in hepatocellular carcinoma: a systematic review and meta-analysis. Hepatol Intl 8(4):493–500. https://doi.org/10.1007/s12072-014-9566-0
38. Huo L, Guo J, Dang Y, Lv J, Zheng Y, Li F, Xie Q, Chen X (2015) Kinetic analysis of dynamic ^{11}C-acetate PET/CT imaging as a potential method for differentiation of hepatocellular carcinoma and benign liver lesions. Theranostics 5(4):371–377. https://doi.org/10.7150/thno.10760
39. Bahler L, Stroek K, Hoekstra JB, Verberne HJ, Holleman F (2016) Metformin-related colonic glucose uptake; potential role for increasing glucose disposal?—a retrospective analysis of ^{18}F-FDG uptake in the colon on PET-CT. Diabetes Res Clin Pract 114:55–63. https://doi.org/10.1016/j.diabres.2016.02.009
40. Russell-Jones D, Cuddihy RM, Hanefeld M, Kumar A, Gonzalez JG, Chan M, Wolka AM, Boardman MK, on behalf of the DURATION-4 Study Group (2012) Efficacy and safety of exenatide once weekly versus metformin, pioglitazone, and sitagliptin used as monotherapy in drug-naive patients with type 2 diabetes (DURATION-4): a 26-week double-blind study. Diabetes Care 35(2):252–258. https://doi.org/10.2337/dc11-1107
41. Lin S, Lin Y, Nery JR, Urich MA, Breschi A, Davis CA, Dobin A, Zaleski C, Beer MA, Chapman WC, Gingeras TR, Ecker JR, Snyder MP (2014) Comparison of the transcriptional landscapes between human and mouse tissues. Proc Nat Acad Sci 111(48):17224–17229. https://doi.org/10.1073/pnas.1413624111